ISSN 1812-5123. Russian Journal of Biomechanics. 2021. Vol. 25, No. 1: 55-66

Russian Journal of Biomechanics
www.biomech.ru

DOI: 10.15593/RJBiomech/2021.1.05

NUMERICAL ANALYSIS OF STRENGTH FOR AN ENDOPROSTHESIS MADE OF A MATERIAL WITH GRADED LATTICE STRUCTURES

V.Sh. Sufiiarov[1], A.V. Orlov[1], A.A. Popovich[1], M.O. Chukovenkova[2], A.V. Soklakov[2], D.S. Mikhaluk[2]

[1] Peter the Great Saint-Petersburg Polytechnic University, 29 Polytechnicheskaya Street, 195251, Saint-Petersburg, Russian Federation
[2] JSC "Center of Engineering Physics Simulation and Analysis", 15/2 Kondratievsky Prospect, 195009, Saint-Petersburg, Russian Federation, e-mail: maria.chukovenkova@multiphysics.ru

Abstract. The most common causes of conducting a hip revision surgery after total hip replacement are aseptic loosening (aseptic instability) of the endoprosthesis, bone destruction as a result of contact with the endoprosthesis, and a periprosthetic fracture. These are the effects of load transfer to the bone tissue in arthroplasty resulting due to the difference in stiffness of the endoprosthesis and the bone. Titanium alloy is widely used in endoprostheses manufacturing because of its high biocompatibility, good wear properties, and corrosion resistance, but such endoprostheses are stiffer than the femur. These problems have aroused interest in searching for the best materials and topology for a femoral implant. Nowadays, additive technology is of great interest as it enables to create materials with graded density. These materials consist of multiple lattice structures with variable parameters and topology. By varying the parameters of lattice structures, one can adjust the mechanical properties of the material as required. These materials find their application in hip endoprostheses manufacturing, allowing to adjust the parameters of the lattice structures and deliver a product with femur-like mechanical properties. The porous structure also ensures bone tissue ingrowth into the prosthesis. The authors designed and simulated an endoprosthesis made of graded density lattice structures with femur-like mechanical properties. Using a numerical simulation software ANSYS Mechanical, authors determined the effect of the topology on the structural behavior of the femur and defined the endoprosthesis-femur combined performance under various load cases.

Key words: endoprosthesis, additive manufacturing, finite element methods, graded material, Ti-6Al-4V.

Vadim Sh. Sufiyarov, Ph.D., Senior Researcher, Peter the Great Saint-Petersburg Polytechnic University, Saint-Petersburg
Aleksey V. Orlov, Scientific Researcher, Peter the Great Saint-Petersburg Polytechnic University, Saint-Petersburg
Anatoliy A. Popovich, Ph.D., Professor, Peter the Great Saint-Petersburg Polytechnic University, Saint-Petersburg
Mariya O. Chukovenkova, Engineer of JSC "Center of Engineering Physics Simulation and Analysis", Saint-Petersburg
Aleksandr V. Soklakov, Head of Group of JSC "Center of Engineering Physics Simulation and Analysis", Saint-Petersburg
Dmitriy S. Mikhalyuk, Director General of JSC "Center of Engineering Physics Simulation and Analysis", Saint-Petersburg

INTRODUCTION

Total hip arthroplasty is replacing hip components with an endoprosthesis. The goal of arthroplasty is to get patients back to their usual lifestyle by recovering the joint function, recovering muscle strength, and relieving pain. Though total hip arthroplasty is one of the most clinically effective operations, with satisfactory clinical outcomes at a follow-up of 15–20 years [18, 19], 10–20% of operations require revision surgery [17]. Common causes for hip revision surgery are aseptic loosening (aseptic instability) of the endoprosthesis [40, 12], bone destruction as a result of contact with the endoprosthesis [12, 26], and a periprosthetic fracture [12, 22, 33]. These are the effects of load transfer to the bone tissue in arthroplasty as a result of the difference in stiffness of the endoprosthesis and the bone [16]. Most hip endoprostheses are made of hard metals, such as a titanium alloy, which is widely used in the manufacture of endoprostheses because of its high biocompatibility, good wear properties, and corrosion resistance [23]. However, such endoprostheses have higher stiffness than the femur [4, 32]. All of the above have promoted interest in searching for the best materials and topology for a femoral implant. In [1], the authors optimized the endoprosthesis topology by reducing its initial volume and obtained a geometry represented as a closed hollow part. However, manufacturing the designed endoprosthesis as one unit is troublesome. Some attempts have been made to reduce the difference in stiffness of the endoprosthesis and the bone by manufacturing endoprostheses with composite and isoelastic stems [15, 34, 35, 41]. Nowadays, additive technology that helps create materials with graded density is increasingly used for improving the topology of endoprostheses. Such materials represent multiple lattice structures with various parameters and topology, which can be used to create designs with desired mechanical characteristics. By adjusting the topology of the lattice structures, one can control the mechanical characteristics of the manufactured product. The periodic structure of these materials is favorable to manufacturing endoprostheses, while the porous structure ensures bone tissue ingrowth into the prosthesis [3, 20, 31, 38]. In [22, 23, 25], the behavior of endoprostheses made of graded materials under different loading conditions is analyzed. One of the effective tools to design graded materials is simulation. The objective of this paper is to use simulation tools to determine the effect of the topology on the structural behavior of the femur and the endoprosthesis–femur joint deformation.

MATERIALS AND METHODS

For simulation purposes, the ANSYS 19.1 finite element analysis package was used. The geometries of lattice structures were prepared in the ANSYS SpaceClaim CAD module. The mesh was generated using ANSYS Meshing. Problem setup, solution, and post-processing of the results were performed in ANSYS Mechanical.

The authors analyzed the following designs: a femur without an endoprosthesis, a femur with an endoprosthesis made of a solid material, and a femur with an endoprosthesis made of a graded material.

The results of analyzing the femur without an endoprosthesis were used as reference data for measuring changes in post total hip arthroplasty load transfer in the bone. To analyze the stress-strain behavior of the bone without endoprosthesis, a high-precision 3D Computed tomography anatomical model of the femur was used [24]. Computed tomography helps create 3D models of organs, which are highly accurate in shape and properties of soft and bone tissues. The human femur has three specific regions that are different in structure and, thus, in mechanical properties: cortical (compact) bone, trabecular (cancellous) bone, and bone marrow (see Fig. 1) [8].

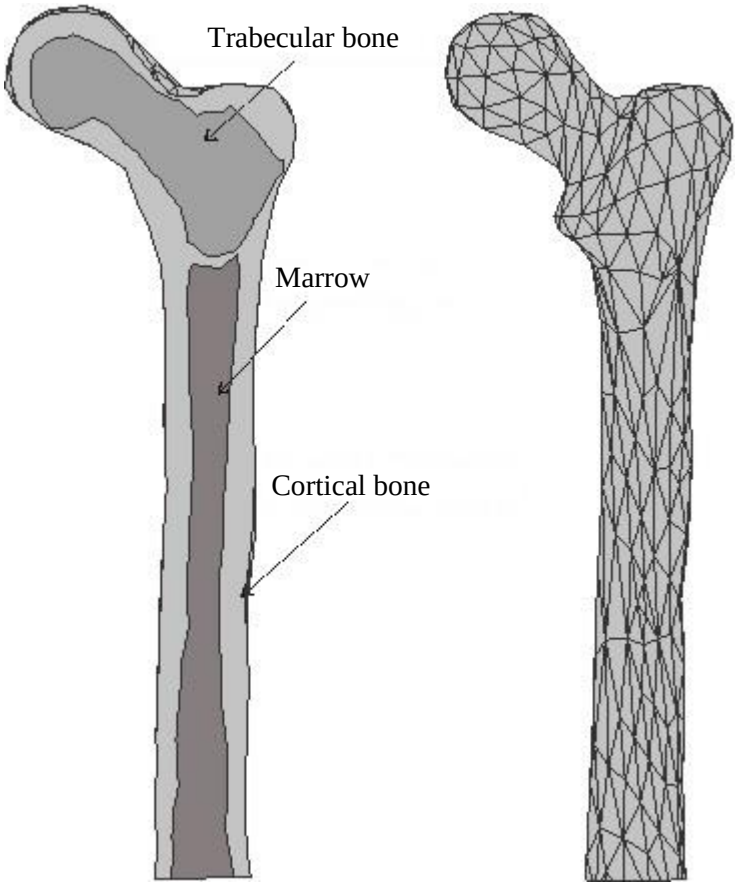

Fig. 1. Anatomical computer model of the femur

Statement of the problem

The designs of new endoprostheses are subject to preclinical trials to prevent any damage during operation. Finite element simulation helps predict the stress-strain behavior of the endoprosthesis and improve its topology to prevent adverse effects.

Stiffness of the bone–endoprosthesis system, bone strength, and endoprosthesis strength were selected as criteria for comparing an endoprosthesis made of a solid material and an endoprosthesis made of a graded material.

The experimental structural testing of endoprostheses is carried out as per GOST R ISO 7206-4-2012 [13]. A cyclic load is applied to the femoral head to cause axial compression, biplanar bending, and rotation until the head breaks or executes a given number of cycles. Actual loads differ from those specified in the standard [5]. Therefore, in the current paper, the authors studied main load cases that represent the most common in-vivo loading conditions, namely, quiet upright standing, walking, stair climbing. Therefore, in the current paper, the authors studied main load cases that represent the most common in-vivo loading conditions, namely, quiet upright standing, walking, stair climbing. The case of jogging at a speed of 7 km/h was also studied, since this type of physical activity is very popular among post total hip arthroplasty patients. Additionally, paper [5] provides a combined load case that was also used for the evaluation. In this load case the angle of the joint reaction force positioning the femur 20º in the transverse plane to assess its effect on the overall strain distribution, and the action of the three major muscle groups, the adbuctors, the vastus lateralis and the iliopsoas, was applied.

The designed model of the bone–endoprosthesis system and its loading configuration are shown in Fig. 2. To simulate a routine arthrotomy, the femoral model was incised along the greater trochanter, and the endoprosthesis model was inserted into the femur.

Endoprosthesis loading is analyzed in coordinates relative to the right femur. The coordinate origin is centered on the femoral head. Muscular loads on the femur are also taken into account. Data on the loads arising from the analyzed types of activity was taken from [30]. The bone–endoprosthesis system is fixed to the lower surface of the femur in all directions. The node at the location of hip contact, i.e., where the hip contact force was applied, was constrained such that this node could only deflect along a local *z* axis towards the posterior condylar center [36].

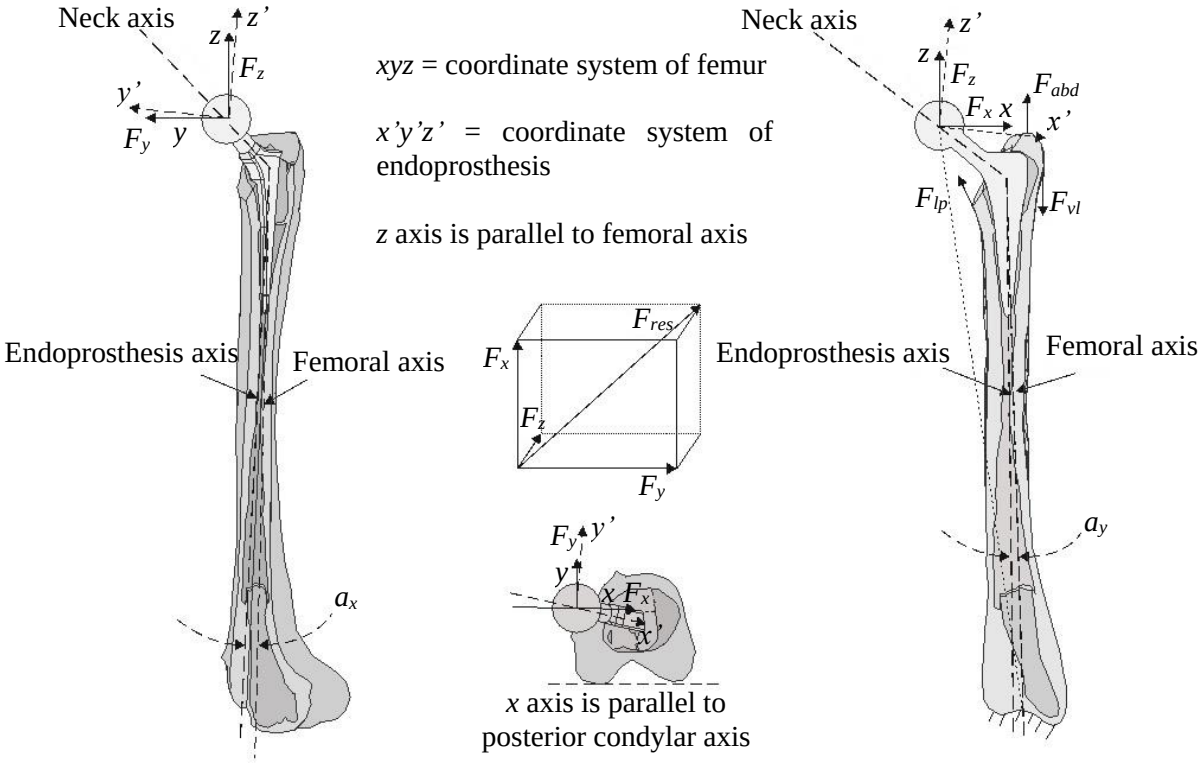

Fig. 2. Model and loading configuration of the bone–endoprosthesis system

Table 1

Values and directions of forces and moments

Load case	Load position	F_x, N	F_y, N	F_z, N	F_{res}, N
Combined (*LC*1)	Femoral head	262	-36	-681	730
	Abductor	-103	0	282	300
	Ilipsoas	-29	136	127	188
	Vastus lateralis	0	0	-292	292
Taking upright position (*LC*2)	Femoral head	650	204	-1.428	1.582
Upright standing (*LC*3)	Femoral head	576	121	-1.947	2.034
Stair climbing (*LC*4)	Femoral head	712	657	-2.000	3.054
Jogging (*LC*5)	Femoral head	774	771	-2.852	3.054

Table 2

Stress-strain properties of the femur regions

	Cortical bone	Trabecular bone	Marrow
Young's modulus, GPa	20.0	2.0	0.3
Poisson's ratio	0.3	0.3	0.45

For stress transfer between the endoprosthesis and the femur, linear contacts the open/closed status of which remains unchanged during the analysis were used – it is necessary to avoid relative movements between the endoprosthesis and the femur in real life. The

endoprosthesis was simulated with VT6 alloy the mechanical properties of which are given in the Table 2 [39].

Design of an endoprosthesis made of a graded material

To manufacture an endoprosthesis with femur-like mechanical characteristics, it is necessary to determine appropriate lattice structures the effective properties of which match the mechanical properties of the bone. This will give strength to the bone attached to the endoprosthesis. Selection of the appropriate lattice structures was based on the following parameters: Young's modulus, pore size, tensile strength. For this study, the authors selected six representative topologies of lattice structures: N, MN, CoRN, CrMN, CoCrRN, and CoCrRMN (see Fig. 3). The authors defined a system of cell configuration naming according to the directions of the struts: N means diagonal struts; R means the central vertical strut; Co means struts located on the four vertical edges of the unit cell; Cr means struts running diagonally from the vertical faces of the unit cell; M means struts running from the center of the unit cell to the midpoints of the horizontal edges. The topologies of the structures are a combination of multidirectional struts with a constant generator N. The unit cell parameters are 2.5 * 2.5 * 2.5 mm at strut thicknesses of 0.3 mm, 0.4 mm, 0.6 mm, 0.8 mm, 1 mm.

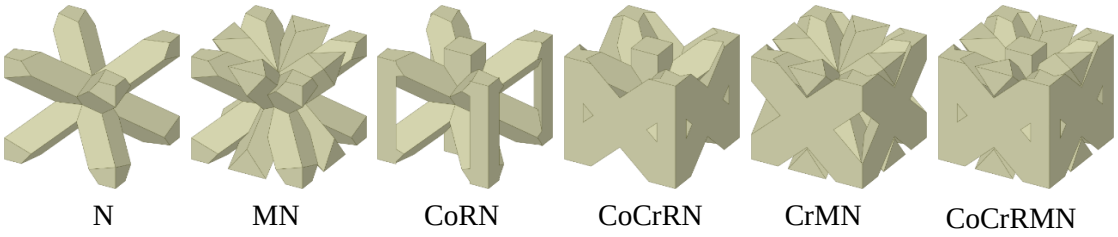

Fig. 3. Configurations of lattice structures

The effective mechanical properties of lattice structures were determined by simulating a compression test [39]. The authors analyzed a wide range of elastic and plastic stresses and strains on a curve and found tensile strength for the lattice structure.

Table 3

Linear elastic material model parameters of the VT6 material

Young's modulus, GPa	113
Poisson's ratio	0,36

Table 4

VT6 characteristics for a multilinear plastic material model

ε, mm/mm	0	0.00096	0.00349	0.00620	0.00894	0.011729	0.01738	0.02025	0.06296
σ, MPa	684.5	915.1	970.4	1006.8	1034.0	1054.3	1084.5	1096.1	1177.6

The plastic material model used to simulate uniaxial tension is multilinear. The multilinear plastic material model takes the following input parameters: Young's modulus *E*, Poisson's ratio μ, and plastic stress σ–plastic strain ε relationship. Plastic strain is important to take into account when simulating the actual mechanical properties of the strut material and obtaining a wide range of effective mechanical properties of the structures. The material used to manufacture the endoprosthesis struts is titanium alloy VT6. The mechanical properties of VT6 were determined as a result of a tensile test carried out by the authors on the round test specimens manufactured by selective laser melting and subsequent heat treatment [28, 29]. The mechanical properties of VT6 are shown in Tables 3 and 4.

The pore size lies in the range of 0.4–0.8 mm for the cortical bone and 0.8–1.2 mm for the trabecular bone [21, 37]. Large pores (0.8–1.2 mm) function as a drain in the prosthesis by supplying organic matter into the endoprosthesis, while small pores (0.4–0.8 mm) ensure the articulation of the prosthesis and the bone. Here, we needed to select a topology and a strut size according to the established criteria for the pore sizes. The pore size in the models analyzed is determined by the size of a sphere inscribed with the lattice structure; this approach has been used previously [7].

We selected lattice structures with the following values of the effective Young's modulus: 14–28 GPa for the cortical bone and 0.1–4 GPa for the trabecular bone [10, 11, 14].

Table 5

Mechanical properties of the selected lattice structures

	VT6	Cortical bone	CoCrRN(0.45)+ CoCrRMN(0.40)	CoCrRN(0.40)+ CoCrRMN(0.45)	Trabecular bone	N(0.48)	MN(0.30)	CrMN (0.35)
Young's modulus, GPa	113.2	14.0–27.0	14.5	14.6	0.1–4.0	2.5	0.92	4.0
Tensile strength, GPa	1177.6	100.0–200.0	167.0	185.0	10.0–130.0	86.4	35.2	102.2

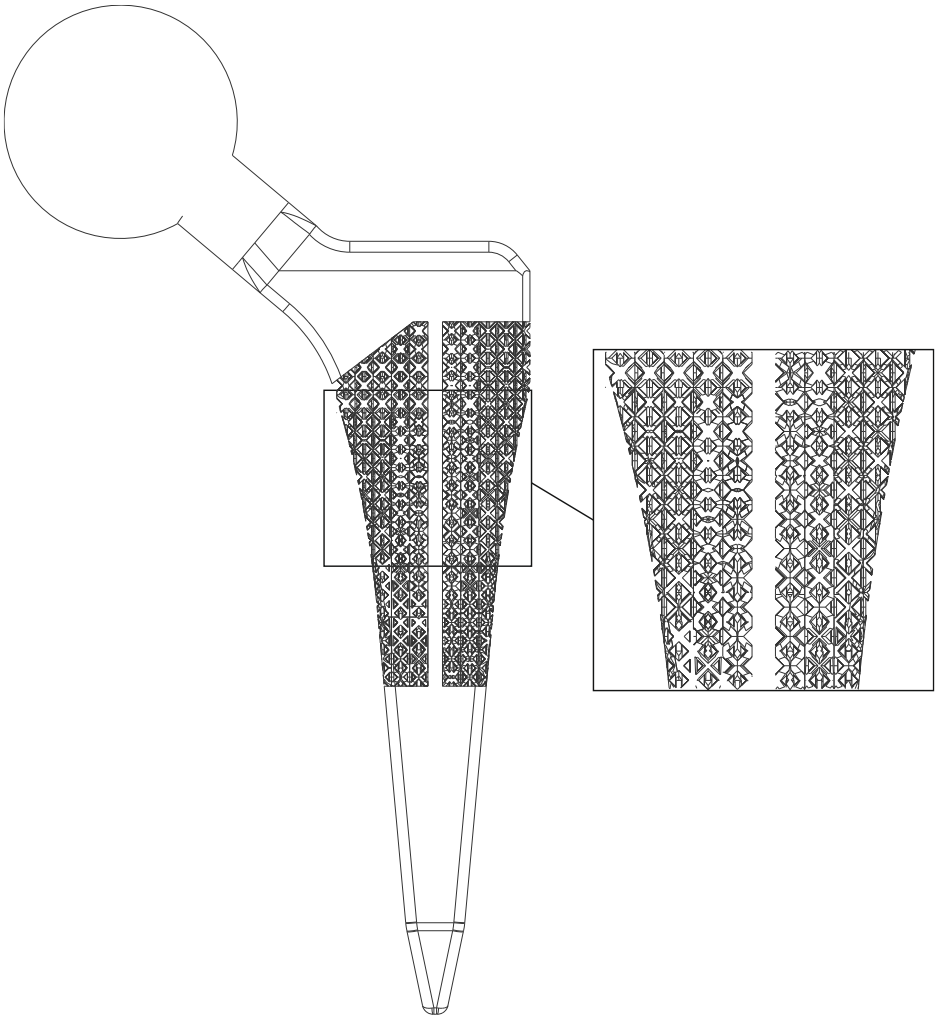

Fig. 4. Model of endoprosthesis made of a material with graded density

The values of the effective tensile strength for the trabecular bone are 10–130 MPa and 100–200 MPa for the cortical bone [10, 21, 37]. Here, we needed to select a topology and a strut size according to the established criteria for tensile strength.

Table 5 shows the values of Young's modulus and tensile strength for VT6, the cortical bone, the trabecular bone, and the selected lattice structures.

In Fig. 4 shows the designed model of an endoprosthesis made of a graded material and the bone–prosthesis system made of a graded material. To simulate a graded material with femur-like mechanical properties, we used the following lattice structures: CoCrRMN with a strut thickness of 0.4 mm and CoCrRN with a strut thickness of 0.45 mm; CoCrRN with a strut thickness of 0.4 mm and CoCrRMN with a strut thickness of 0.45 mm; CoCrRN with a strut thickness of 0.4 mm and CoCrRMN with a strut thickness of 0.48 mm for the cortical bone; N with a strut thickness of 0.48 and MN with a strut thickness of 0.3; MN with a strut thickness of 0.3 mm and CrMN with a strut thickness of 0.35 mm for the trabecular bone.

RESULTS

Using the finite element method, we analyzed the effect of different endoprosthesis models on the stress-strain behavior of the femur for different types of human activity, such as walking, upright standing, taking upright position, stair climbing, and jogging. The study was performed for a femur without an endoprosthesis, a femur with an endoprosthesis made of a solid material, and a femur with an endoprosthesis made of a graded material.

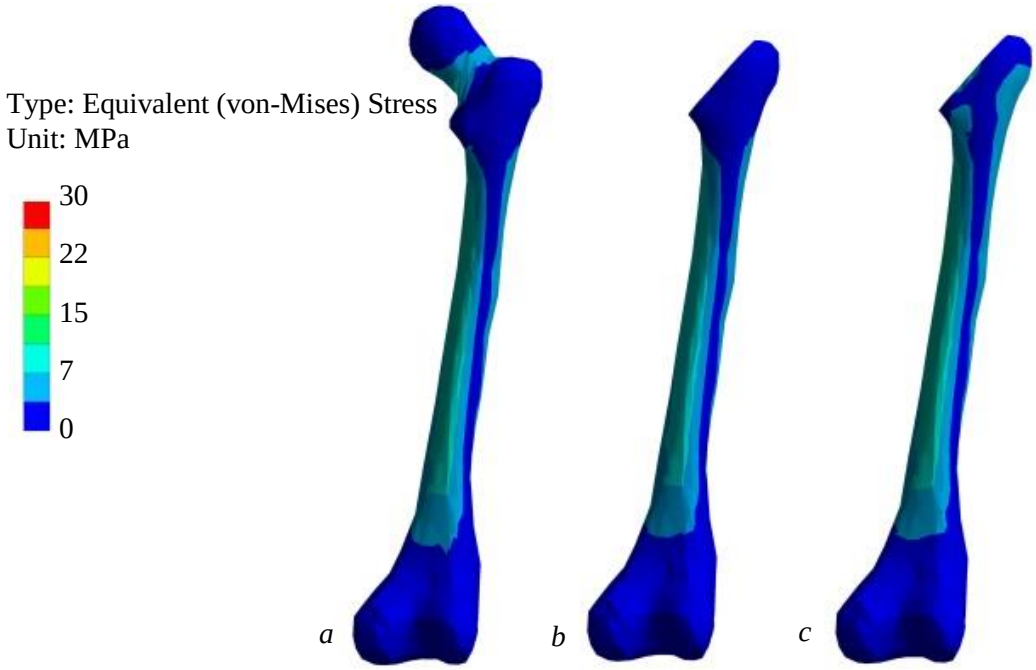

Fig. 5. Von Mises stress fields (MPa) for a femur without an endoprosthesis *a*, a femur with a solid-material endoprosthesis *b*, a femur with a graded-material endoprosthesis *c* under combined loads

In Fig. 5 shows von Mises stress fields in the femur with a solid-material endoprosthesis and the femur with a graded-material endoprosthesis under combined loads. When the bone–endoprosthesis system is subject to loads, the endoprosthesis topology has no observable effect on the overall stress state of the femur. However, where the endoprosthesis from a solid material articulates with the femur surface, local strain reduction is observed in the upper part of the cortical bone. Due to its high stiffness, the endoprosthesis takes the major load and does not transfer it to the cortical bone, which reduces strains in the bone (see Fig. 6). This adverse effect is called stress shielding [9, 27]. By Wolff's law [42], changes in

the functional loading of the bone cause its adaptive remodeling, which in the case of a decrease in the active load results in the weakening and further destruction of the bone tissue.

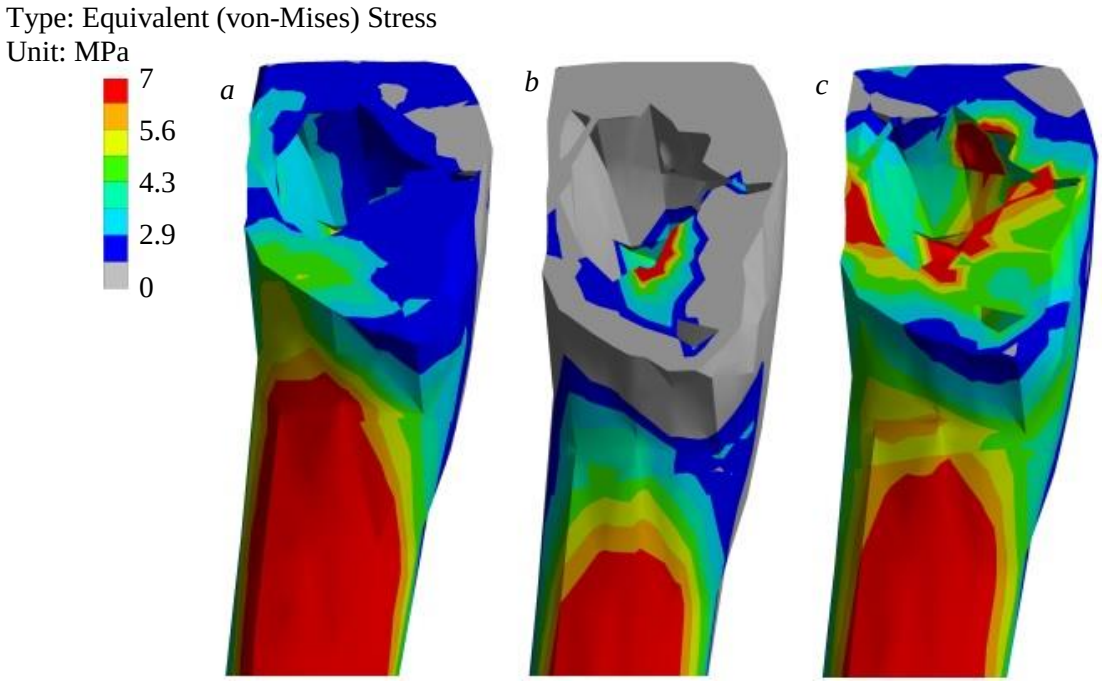

Fig. 6. Von Mises stress fields (MPa) for the upper part of a femur without an endoprosthesis *a*, a femur with a solid-material endoprosthesis *b*, a femur with a graded-material endoprosthesis *c* under combined loads

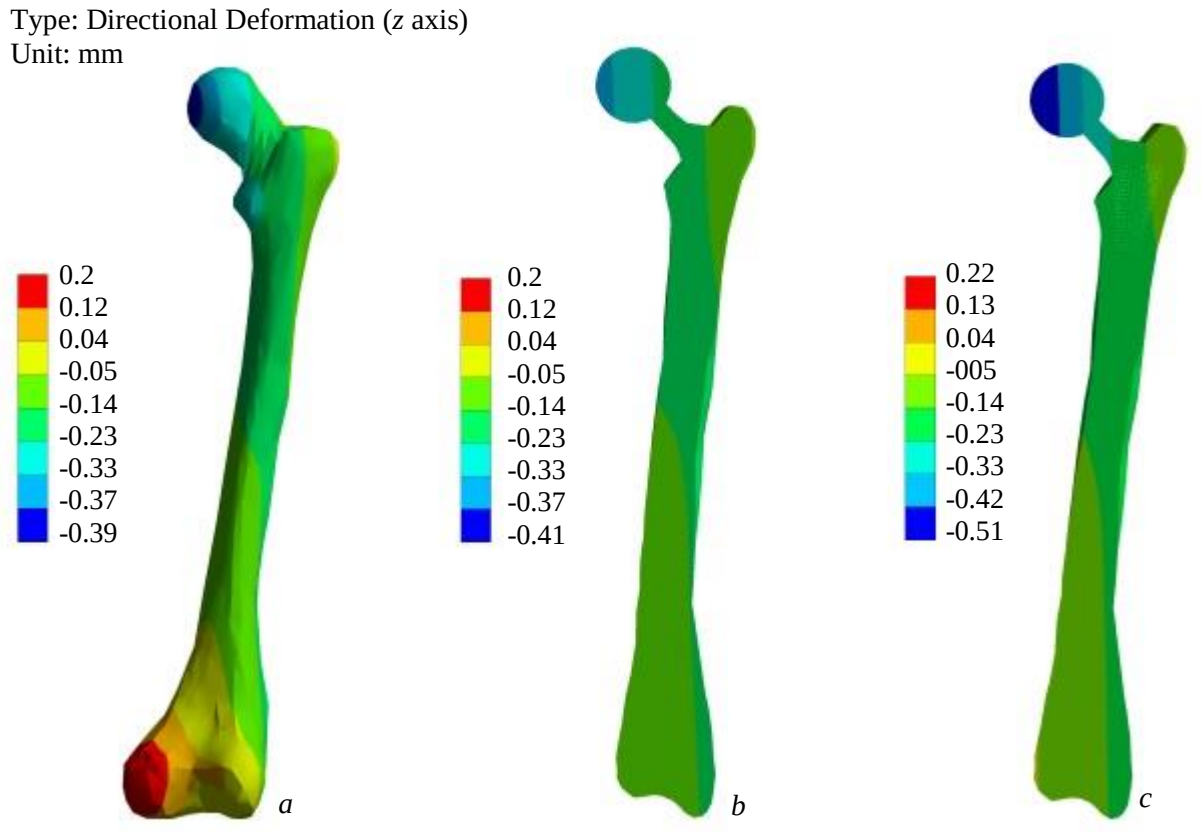

Fig. 7. Displacement fields (mm) for a femur without an endoprosthesis *a*, a femur with a solid-material endoprosthesis *b*, a femur with a graded-material endoprosthesis *c* under combined loads

ISSN 1812-5123. Russian Journal of Biomechanics. 2021. Vol. 25, No. 1: 55-66

Fig. 6 shows von Mises stress fields for the upper part of the cortical bone in a femur without an endoprosthesis, a femur with a solid-material endoprosthesis, and a femur with a graded-material endoprosthesis.

The analysis shows that strains in the femur with a graded-material endoprosthesis are higher than those in the femur with a solid-material endoprosthesis and do not exceed those in the femur without an endoprosthesis. This reduces the risk of stress shielding and ensures femoral strength.

Table 6

The maximum values of the bone (endoprosthesis) head displacements in *x*, *y* and *z* directions (mm)

		Femur bone without endoprosthesis	Femur bone with solid-material endoprosthesis	Femur bone with graded-material endoprosthesis
*LC*1	*Ox*	0.58	0.63	0.68
	Oy	0.36	0.37	0.36
	Oz	0.39	0.41	0.51
*LC*2	*Ox*	1.26	1.35	1.47
	Oy	0.77	0.80	0.78
	Oz	0.84	0.89	1.11
*LC*3	*Ox*	1.62	1.73	1.90
	Oy	1.00	1.03	1.01
	Oz	1.08	1.15	1.42
*LC*4	*Ox*	1.76	1.90	2.07
	Oy	1.11	1.15	1.12
	Oz	1.18	1.27	1.56
*LC*5	*Ox*	2.44	2.62	2.86
	Oy	1.50	1.55	1.51
	Oz	1.62	1.75	2.14

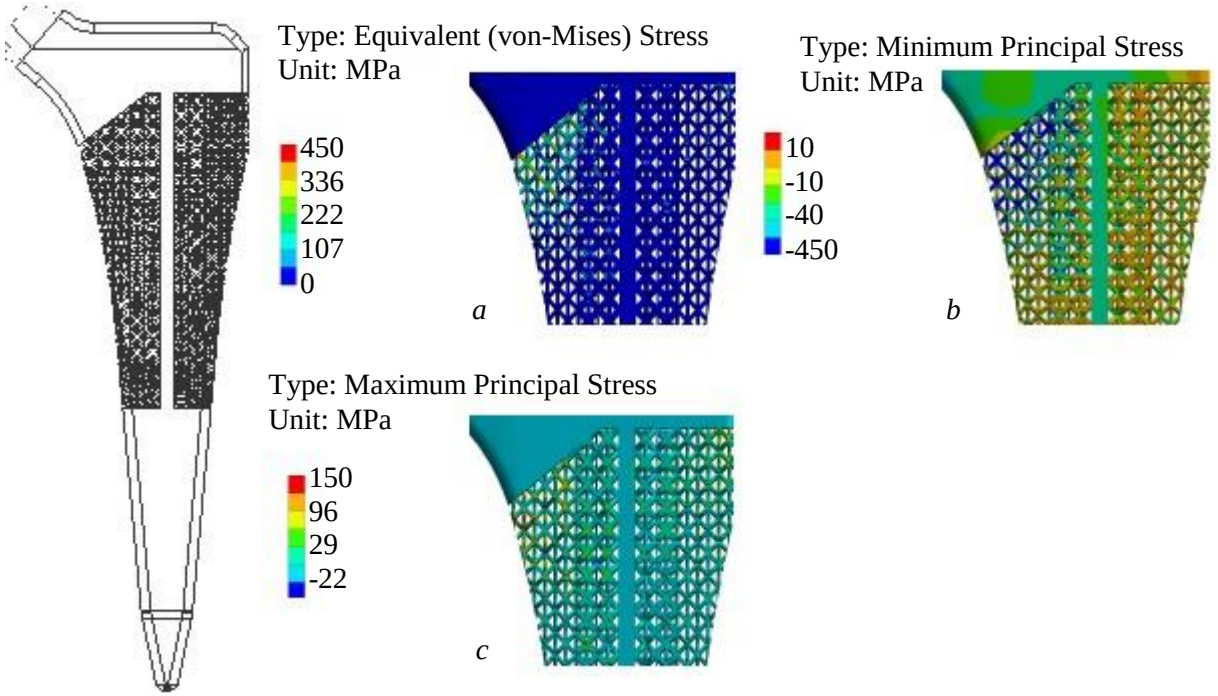

Fig. 8. Von Mises stress fields *a*, maximum tension *b* and maximum compression *c* stress fields (MPa) for a graded-material endoprosthesis under maximum load

In Fig. 7 shows displacement fields for a femur without an endoprosthesis, a femur with a solid-material endoprosthesis, and a femur with a graded-material endoprosthesis under combined loads. The displacement values at the head top are as follows: 0.39 mm for a solid bone, 0.41 mm for a bone–solid endoprosthesis system, 0.51 mm for a bone-graded endoprosthesis system.

Maximum values of the displacement in *x, y, z* directions for all load cases are presented in Table 6.

Displacement values obtained in the current research are of the same order as the values of other studies [2, 6]. Differences could be caused by differences in boundary conditions or by difference in bone material model used.

Fig. 8 shows von Mises stress fields, maximum tension and maximum compression stress fields for an endoprosthesis made of a graded material under maximum jogging load.

Based on the simulation, strains in the endoprosthesis made of a graded material are lower than yield strength of VT6. The margin of safety in the maximum load case is 2. Therefore, the lattice structure strength of a graded-material endoprosthesis is ensured for all of the analyzed types of activity.

CONCLUSIONS

The objective of this paper was to investigate the effect of the endoprosthesis topology on the stress-strain behavior of the femur. Two endoprosthesis topologies were analyzed: an endoprosthesis made of a solid material and an endoprosthesis made of a material with graded density.

A model of a graded-material endoprosthesis was designed. The effective properties of the lattice structures that form the graded material match the mechanical properties of the femur, which ensures the bone strength as it interacts with the endoprosthesis. Selection of the appropriate lattice structures was based on the following parameters: Young's modulus, pore size, tensile strength. The porous structure of the graded material ensures bone tissue ingrowth into the prosthesis.

Load cases for walking, quiet upright standing, taking upright position, stair climbing, and jogging were analyzed. For a more accurate analysis of the load cases, forces arising under loads placed by major muscles on the femur were taken into account.

The simulation shows that an endoprosthesis made of a graded material can carry loads arising from standard types of human activity. It was also determined that an endoprosthesis made of a graded material has lower stiffness than that of a solid material, which helps reduce the risk of aseptic loosening and prevent the need for revision surgery.

REFERENCES

1. Adam F., Hammer D.S., Pfautsch S., Westermann K. Early failure of a press-fit carbon fiber hip prosthesis with a smooth surface. *Journal of Arthroplasty*, 2002, vol. 7, pp. 217-223.
2. Andreaus U., Colloca M., Toscano A. Mechanical behaviour of physiological and prosthesized human femurs during stair climbing: A comparative analysis via 3D numerical simulation. *Minerva Ortopedica Traumatologica*, 2008, vol. 59, no. 4, pp. 213-220.
3. Arabnejad Khanoki S., Pasini D. Multiscale design and multiobjective optimization of orthopedic hip implants with functionally graded cellular material. *Journal of Biomechanical Engineering*, 2012, vol. 134, no. 3, pp. 1-45.
4. Behrens B., Wirth C.J., Windhagen H., Nolte I., Meyer-Lindenberg A., Bouguecha A. Numerical investigations of stress shielding in total hip prostheses. *Journal of Engineering in Medicine*, 2008, vol. 222, pp. 593-600.
5. Bergmann G., Bender A., Dymke J., Duda G. Damm standardized loads acting in hip implants. *PLoS ONE*, 2016, vol. 22, pp. 462-471.

6. Björnsdóttir M. Influence of muscle forces on stresses in the human femur, available at: https://www.diva-portal.org/smash/get/diva2:839895/FULLTEXT01.pdf (accessed 5 March 2021).
7. Chappard C. et al. 3D characterization of pores in the cortical bone of human femur in the elderly at different locations as determined by synchrotron micro-computed tomography images. *Osteoporosis International*, 2013, vol. 24, pp. 1023-1033.
8. Currey J.D. Bones structure and mechanics. Princeton University Press, 2002, 436 p.
9. Dammak M., Shirazi-Adl A., Zukor D.J. Analysis of cementless implants using interface nonlinear friction-experimental and finite element studies. *Journal of Biomechanics*, 1997, vol. 30, pp. 121-129.
10. Dumas M., Terriault P., Brailovski V. Modelling and characterization of a porosity graded lattice structure for additively manufactured biomaterials. *Material Design*, 2017, vol. 121, pp. 383-392.
11. Goldstein S.A. The mechanical properties of trabecular bone: dependence on anatomic location and function. *Journal of Biomechanics*, 1987, vol. 20, pp. 1055-1061.
12. Goodnough L.H., Finlay A.K., Huddleston J.I., Goodman S.B., Maloney W.J., Amanatullah D.F. Obesity is independently associated with early aseptic loosening in primary total hip arthroplasty. *Journal of Arthroplasty*, 2018, vol. 33, pp. 882-886.
13. GOST R ISO 7206-4-2012. Implants for surgery. Partial and total hip joint prostheses. Part 4. Determination of endurance properties and performance of stemmed femoral components. (*in Russian*).
14. Hollister S.J., Lin C.Y., Saito E., Lin C.Y., Schek R.D., Taboas J.M., Williams J.M., Partee B., Flanagan C.L., Diggs A., Wilke E.N., Van Lenthe G.H., Müller R., Wirtz T., Das S., Feinberg S.E., Krebsbach P.H. Engineering craniofacial scaffolds. *Orthodontics Craniofacial Research*, 2005, vol. 8, pp. 162-173.
15. Jetté B., Brailovski V., Dumas M., Simoneau C., Terriault P. Femoral stem incorporating a diamond cubic lattice structure: Design, manufacture and testing. *Journal of the Mechanical Behavior of Biomedical Materials*, 2018, vol. 77, pp. 58-72.
16. Katoozian H., Davy D.T., Arshi A., Saadati U. Material optimization offemoral component oftotal hip prosthesis using fiber reinforced polymeric composites. *Medical Engineering & Physics*, 2001, vol. 23, pp. 505-511.
17. Kurtz S., Ong K., Lau E., Mowat F., Halpern M. Projections of primary and revision hip and knee arthroplasty in the United States from 2005 to 2030. *Journal of Bone and Joint Surgery*, 2007, vol. 89, pp. 780-785.
18. Laupacis A., Bourne R., Rorabeck C., et al. The effect of elective total hip replacement on health-related quality of life. *Journal of Bone and Joint Surgery*, 1993, vol. 75, pp. 1619-1626.
19. Learmonth I.D., Young C., Rorabeck C. The operation of the century: total hip replacement. *Lancet*, 2007, vol. 370, pp. 1508-1519.
20. Limmahakhun S., Oloyede A., Sitthiseripratip K., Xiao Y., Yan C. 3D-printed cellular structures for bone biomimetic implants. *Additive Manufacturing*, 2017, vol. 15, pp. 93-101.
21. Liu F., Zhang D.Z., Zhang P., Zhao M., Jafar S. Mechanical properties of optimized diamond lattice structure for bone scaffolds fabricated via selective laser melting. *Materials (Basel)*, 2018, vol. 11, pp. 383-392.
22. Long M., Rack H. Titanium alloys in total joint replacement – a materials science perspective. *Biomaterials*, 1998, vol. 19, pp. 1621-1639.
23. Lynch M.E., Mordasky M., Cheng L., To A., Design, testing, and mechanical behavior of additively manufactured casing with optimized lattice structure. *Additive Manufacturin*, 2018, vol. 22, pp. 462-471.
24. Makarov S.N., Noetscher G.M., Yanamadala J., Piazza M.W., Louie S., Prokop A., Nazarian A., Nummenmaa A. Virtual human models for electromagnetic studies and their applications. *IEEE Reviews in Biomedical Engineering*, 2017, vol. 10, pp. 95-121.
25. Mehboob H., Tarlochan F., Mehboob A., Chang S.-H. Finite element modelling and characterization of 3D cellular microstructures for the design of a cementless biomimetic porous hip stem. *Materials & Design*, 2018, vol. 149, pp. 101-112.
26. Miettinen S.S.A., Mäkinen T.J., Kostensalo I., et al. Risk factors for intraoperative calcar fracture in cementless total hip arthroplasty. *Acta Orthopaedica*, 2016, vol. 87, pp. 113-119.
27. Noyama Y., Miura T., Ishimoto T., Itaya T., Niinomi M., Nakano T. Bone loss and reduced bone quality of the human femur after total hip arthroplasty under stress-shielding effects by titanium-based implant. *Materials Transactions*, 2012, vol. 53, pp. 565-570.
28. Orlov A.V., Sufiiarov V.S., Borisov E.V, Polozov I.A., Masaylo D.V., Popovich A.A., Chukovenkova M.O., Soklakov A.V., Mikhaluk D.S. Numerical simulation of the inelastic behavior of a structurally graded material. *Letters on materials*, 2019, vol. 9, pp. 97-102.
29. Popovich A., Sufiiarov V., Borisov E., Polozov I. Microstructure and mechanical properties of Ti-6AL-4V manufactured by SLM. *Key Engineering Materials*, 2015, vol. 651-653, pp. 677-682.
30. Popovich A., Sufiiarov V., Polozov I., Borisov E., Masaylo D. Producing hip implants of titanium alloys by additive manufacturing. *Journal of Bioprinting*, 2016, vol. 2, pp. 78-84.

31. Popovich A.A., Sufiiarov V.S., Polozov I.A., Borisov E.V., Masaylo D.V., Vopilovskiy P.N., Sharonov A.A., Tikhilov R.M., Tsybin A.V., Kovalenko A.N., Bilyk S.S. Use of additive techniques for preparing individual components of titanium alloy joint endoprostheses. *Biomedical Engineering*, 2016, vol. 50, pp. 202-205.
32. Ridzwan M., Shuib S., Hassan A., Shokri A., Ibrahim M. Optimization in implant topology to reduce stress shielding problem. *Journal of Apllied Sciences*, 2006, vol. 6, pp. 2768-2773.
33. Sidler-Maier C.C., Waddell J.P. Incidence and predisposing factors of periprosthetic proximal femoral fractures: a literature review. *International Orthopaedics*, 2015, vol. 39, pp. 1673-1682.
34. Simoes J.A., Marques A.T. Design of a composite hip femoral prosthesis. *Materials and Design*, 2005, vol. 26, pp. 391-401.
35. Simoes J.A., Marques A.T. Determination of stiffness properties of braided composites for the design of a hip prosthesis. *Composites Part A: Applied Science and Manufacturing*, 2001, vol. 32, pp. 655-662.
36. Speirs A.D., Heller M.O., Duda G.N., Taylor W.R. Physiologically based boundary conditions in finite element modelling. *Journal of Biomechanics*, 2007, vol. 40, no. 10, pp. 2318-2323.
37. Stein M.S. et al. An automated analysis of intracortical porosity in human femoral bone across age. *Journal of Bone and Mineral Research*, 1999, vol. 14, pp. 624-632.
38. Sufiiarov V.Sh., Borisov E.V., Polozov I.A., Masailo D.V. Control of structure formation in selective laser melting process. *Tsvetnye Metally*, 2018, vol. 7, pp. 68-74.
39. Sufiyarov V.S., Borisov E.V. Effect of heat treatment modes on the structure and properties of alloy VT6 after selective laser melting. *Metal Science and Heat Treatment*, 2019, vol. 60, pp.745-748.
40. Traina F., De Fine M., Bordini B., Toni A. Risk factors for ceramic liner fracture after total hip arthroplasty. *HIP International*, 2012, vol. 22, pp. 607-614.
41. Trebse R., Milosev L., Kovac S., Mikek M., Pisot V. Poor results from the isoelastic total hip replacement. *Acta Orthopaedica*, 2005, vol. 76, pp. 169-176.
42. Wolff J. Berdieinnere architectur der knochenundihre bedeutung fur die fragevom knochenwachstum. *Virchow's Archive*, 1870, vol. 50, pp. 389-450.

Recieved 30 September 2019